THE ASTROPHYSICAL JOURNAL, 448:734–741, 1995 August 1

EFFECTS OF PRESSURE AND RESISTIVITY ON THE AMBIPOLAR DIFFUSION SINGULARITY: TOO LITTLE, TOO LATE

AXEL BRANDENBURG
Advanced Study Program & High Altitude Observatory, National Center for Atmospheric Research,[1] P.O. Box 3000, Boulder, CO 8037-3000
AND
ELLEN G. ZWEIBEL[2]
Joint Institute for Laboratory Astrophysics, University of Colorado and National Institute of Standards and Technology, Boulder, CO 80309-0440
Received 1994 October 7; accepted 1995 February 13

ABSTRACT

Ambipolar diffusion, or ion-neutral drift, can lead to steepening of the magnetic field profile and even to the formation of a singularity in the current density. These results are based on an approximate treatment of ambipolar drift in which the ion pressure is assumed vanishingly small and the frictional coupling is assumed to be very strong, so that the medium can be treated as a single fluid. This steepening, if it really occurs, must act to facilitate magnetic reconnection in the interstellar medium, and so could have important consequences for the structure and evolution of the galactic magnetic field on both global and local scales.

In actuality, the formation of a singularity must be prevented by physical effects omitted by the strong coupling approximation. In this paper we solve the coupled equations for charged and neutral fluids in a simple slab geometry, which was previously shown to evolve to a singularity in the strong coupling approximation. We show that both ion pressure and resistivity play a role in removing the singularity, but that, for parameters characteristic of the interstellar medium, the peak current density is nearly independent of ion pressure and scales inversely with resistivity. The current gradient length scale, however, does depend on ion pressure. In the end, effects outside the fluid approximation, such as the finite ion gyroradius, impose the strictest limit on the evolution of the magnetic profile.

Subject headings: diffusion — ISM: magnetic fields — MHD

1. INTRODUCTION

In weakly ionized gases, such as the cold, dense portions of the interstellar medium, the magnetic field, which is carried by the ions, can slip or "diffuse" through the neutral gas. The process is usually called ambipolar diffusion (e.g., Spitzer 1978). It has been investigated primarily as a mechanism for the escape of magnetic flux from dense clouds, as originally proposed by Mestel & Spitzer (1956), and for the damping of hydromagnetic fluctuations (Kulsrud & Pearce 1969); see McKee et al. (1993) for a recent review of these processes.

When the ionization fraction is low and the momentum-exchange time between ions and neutrals is short, it is natural to treat ambipolar drift in the strong coupling approximation (Shu 1983). The essence of this approximation is that the ion-neutral drift velocity, $\boldsymbol{u}_i - \boldsymbol{u}_n$, is balanced by the Lorentz force, leading to terms in the magnetic induction equation which resemble nonlinear diffusion, with a diffusion coefficient proportional to the square of the magnetic field strength.

It is well known that sharp fronts can form and propagate in the presence of nonlinear diffusion (e.g., Zeldovich & Raizer 1967), and we have recently carried out a preliminary investigation of this process in the interstellar medium (Brandenburg & Zweibel 1994, hereafter BZ). We found that if the field has a null and the medium is static, the magnetic profile in the vicinity of the null relaxes to a $z^{1/3}$ profile (where z measures the distance from the null); the corresponding electric current density is infinite. If the field does not have a null but is forced by a sheared velocity field, sharp current profiles also develop, although the current does not formally become singular. Effects of this kind were also seen by Proctor & Zweibel (1992) and by Mac Low et al. (1995).

This mechanism for developing sharp structures and large current densities in the interstellar magnetic field seems to us to be of considerable importance. Without such a mechanism, it is difficult to understand how the magnetic field could ever reconnect on astrophysically interesting timescales: the enormous length scales and relatively large electrical conductivities argue for long reconnection times. Only by reducing the magnetic length scale can reconnection times be appreciably shortened.

The strong coupling approximation must break down in the vicinity of a singularity. The purpose of this paper is to investigate this breakdown and to assess how far singularity formation actually proceeds when the assumption of strong coupling is dropped and resistivity is included. We do this by solving the time-dependent, compressible MHD equations for two fluids, one charged and one neutral, which interact with one another through ionization, recombination, and collisional momentum exchange. In § 2 we discuss the basic equations and derive approximate formulae for predicting their behavior. Our basic result is that the $z^{1/3}$ steady solution is replaced by a profile which is linear in z as z approaches zero, so that the current singularity is removed. The location at which the transition from $z^{1/3}$ to z occurs depends primarily on the resistivity, colli-

[1] The National Center for Atmospheric Research is sponsored by the National Science Foundation.
[2] Also at Department of Astrophysical, Planetary, and Atmospheric Sciences, University of Colorado, Boulder, CO 80309.

sion rate, and recombination rate, with all these factors entering because the inductive electric field associated with the inflow must be ohmically driven near the stagnation point, and the advection of ions inward by the flow must be balanced by recombination. If we assume that these parameters have their interstellar values, we find that the peak current density is approximately inversely proportional to the resistivity. Thus, ambipolar drift appears to remain a viable mechanism for promoting magnetic reconnection in the weakly ionized interstellar medium.

2. GOVERNING EQUATIONS AND LIMITING CASES

We consider the relaxation of a slab of weakly ionized fluid containing a straight magnetic field. The electron and ion fluids are well coupled by an ambipolar electric field over length scales of interest (the Debye length is expected to be by far the shortest length scale in the problem), so we treat only two fluids: one charged, the other neutral. For simplicity we consider only one ionized and one neutral species. We assume that all quantities are functions of time t and one space coordinate z and that the magnetic field $\boldsymbol{B}$ points in the x direction. Flow is driven by magnetic and gas pressure gradients and is in the z direction. We simplify the problem by assuming that both the charged and neutral fluids remain isothermal; thus, we assume that radiative cooling dominates compressive and frictional heating. This probably leads to an underestimate of the effects of pressure, but solving the energy equations correctly would complicate an already challenging problem, as it would be necessary to include ohmic heating, viscous heating (from both self- and interspecies collisions), collisional excitation and radiative decay, and heat conduction by the neutrals and ions.

The governing equations are (e.g., Draine 1986)

$$\frac{\partial B}{\partial t} = -\frac{\partial}{\partial z}\left(u_i B - \lambda \frac{\partial B}{\partial z}\right), \tag{1}$$

$$\frac{\partial}{\partial t}(\rho_i u_i) = -\frac{\partial}{\partial z}\left[\rho_i\left(u_i^2 + 2c_i^2 + \nu \frac{\partial u_i}{\partial z}\right) + \frac{1}{8\pi} B^2\right] + F, \tag{2}$$

$$\frac{\partial}{\partial t}(\rho_n u_n) = -\frac{\partial}{\partial z}\left[\rho_n\left(u_n^2 + c_n^2 + \nu \frac{\partial u_n}{\partial z}\right)\right] - F, \tag{3}$$

$$\frac{\partial \rho_i}{\partial t} = -\frac{\partial}{\partial z}(\rho_i u_i) + G, \tag{4}$$

$$\frac{\partial \rho_n}{\partial t} = -\frac{\partial}{\partial z}(\rho_n u_n) - G, \tag{5}$$

where

$$F = -\rho_i \nu_{in}(u_i - u_n) + \zeta \rho_n u_n - \alpha \rho_i^2 u_i, \tag{6}$$

$$G = \zeta \rho_n - \alpha \rho_i^2. \tag{7}$$

Here c is the sound speed $(kT/m)^{1/2}$, ρ is the density, ζ is the cosmic-ray ionization rate, α is the recombination rate per unit volume, and λ and ν are the magnetic diffusivity and the kinematic viscosity, respectively.

In principle, these viscosities should differ from one another and should include the effect of momentum transfer between species over a collisional mean free path. In practice, it will turn out that the dynamics of the neutral fluid is rather unimportant, so the treatment of its viscosity does not matter much. The major role of viscosity in the ion dynamics is numerical stabilization.

The factor of 2 multiplying the ion pressure accounts for electron pressure. The subscripts i and n refer to the ion and neutral components, respectively. The ion-neutral collision frequency is given by $\nu_{in} = \gamma \rho_n$, where γ is the drag coefficient due to the momentum exchange in ion-neutral collisions, and $\gamma = \langle \sigma v \rangle / (m_i + m_n)$, where $\langle \sigma v \rangle$ is the momentum transfer rate, and m_i and m_n are the particle masses of ions and neutrals.

We first review the strong coupling approximation. This consists of taking the ion density to zero in equation (2) everywhere but in the friction term and in assuming that G is the dominant term in equation (4). That is, the Lorentz force is assumed to be balanced by ion-neutral friction, and ionization equilibrium is assumed to hold. Moreover, the neutral pressure P_n is assumed to dominate the magnetic pressure P_M, so the fractional neutral density perturbation required to balance magnetic forces is small, i.e., of order P_M/P_n. This means that the ion pressure perturbation itself is small, so ion pressure gradients are negligible.

This is the essence of the strong coupling approximation. When it is valid, the ion dynamics need not be calculated explicitly, and the neutral dynamics are ignorable. Therefore, the evolution of the magnetic field can be determined from the magnetic induction equation alone. A less restrictive form of the strong coupling approximation would be to neglect ion pressure and inertia, but to include the effect of Lorentz forces (transmitted by friction) on the neutrals. This case is obviously of great interest in the interstellar medium. Applying the strong coupling approximation to the case in which the magnetic field initially has a null at $z = 0$ and setting the magnetic diffusivity $\lambda = 0$, we find that the location of the null is preserved and that the magnetic field profile relaxes to a steady state with $B \propto z^{1/3}$ (BZ). The Lorentz force, and the ion velocity, then go as $z^{-1/3}$. This singularity in u_i (or near singularity, as any resistivity at all will remove the strong current at the origin) means that the ion density must be driven away from ionization equilibrium near the origin. The resulting ion pressure peak formed by the strong convergent flow must become dynamically important near the null. One of the main purposes of this paper is to calculate the effect of ion pressure near the null point.

It is also interesting to consider the opposite limit, in which ionization recombination, and frictional momentum transfer are all negligibly weak. In this case, a steady state is reached (in the nonresistive limit) when ion pressure and magnetic pressure balance each other. The final state can be calculated explicitly for any initial magnetic and ion density profiles using Lagrangian methods. In general, the ion pressure has a peak in the vicinity of the magnetic null. But if slow ionization and recombination are turned on once equilibrium is reached, the ion pressure peak will gradually disappear and the magnetic field profile will approach a step function, with constant positive and negative values on either side of the null. This, of course, is even more singular than the magnetic profiles predicted by the strong coupling approximation. However, we have never seen evolution of this type in our simulations, presumably because ion-neutral friction cannot be neglected in the parameter regime examined.

Returning to the full problem, we solve the equations of motion numerically using the following (nonconservative) formulation:

$$\frac{\partial B}{\partial t} = -u_i \frac{\partial B}{\partial z} - B \frac{\partial u_i}{\partial z} + \lambda \frac{\partial^2 B}{\partial z^2}, \tag{8}$$

$$\frac{\partial u_i}{\partial t} = -u_i \frac{\partial u_i}{\partial z} - 2c_i^2 \frac{\partial \ln \rho_i}{\partial z} - \frac{1}{4\pi} \frac{B}{\rho_i} \frac{\partial B}{\partial z} - \rho_n \left(\gamma + \frac{\zeta}{\rho_i}\right)(u_i - u_n) + \nu \left(\frac{\partial^2 u_i}{\partial z^2} + \frac{\partial u_i}{\partial z} \frac{\partial \ln \rho_i}{\partial z}\right), \quad (9)$$

$$\frac{\partial u_n}{\partial t} = -u_n \frac{\partial u_n}{\partial z} - c_n^2 \frac{\partial \ln \rho_n}{\partial z} + \rho_i \left(\gamma + \alpha \frac{\rho_i}{\rho_n}\right)(u_i - u_n) + \nu \left(\frac{\partial^2 u_n}{\partial z^2} + \frac{\partial u_n}{\partial z} \frac{\partial \ln \rho_n}{\partial z}\right), \quad (10)$$

$$\frac{\partial \ln \rho_i}{\partial t} = -u_i \frac{\partial \ln \rho_i}{\partial z} - \frac{\partial u_i}{\partial z} + \zeta \frac{\rho_n}{\rho_i} - \alpha \rho_i , \quad (11)$$

$$\frac{\partial \ln \rho_n}{\partial t} = -u_n \frac{\partial \ln \rho_n}{\partial z} - \frac{\partial u_n}{\partial z} - \zeta + \alpha \rho_i \frac{\rho_i}{\rho_n} . \quad (12)$$

As boundary conditions, we require that the magnetic field and the velocity vanish at $z = 0$, i.e., $B = u_i = u_n = 0$. In order to be able to approach a steady state, we prescribe the densities and magnetic field on the outer boundary $z = L$, where L is the length of the computational domain, i.e., $B = B_0$, $\rho_i = \rho_{i0}$, and $\rho_n = \rho_{n0}$. As an initial condition, we choose $B = B_0 z/L$, $u_i = u_n = 0$, $\rho_i = \rho_{i0}$, and $\rho_n = \rho_{n0}$.

We solve the system of equations using a third-order Hyman scheme for the time step and second-order finite differences on a uniform mesh. We choose a value of λ that is close to the minimum value required for numerical stability. This value is given by the maximum grid Reynolds number for the magnetic field, $R_m^{\rm grid} = c\,\delta x/\lambda$, where δx is the mesh width and $c = \max(c_i, c_n)$. In practice, $R_m^{\rm grid}$ cannot exceed the value of ~ 4. In all cases presented here we used 1024 mesh points, i.e., $\lambda = 2.4 \times 10^{-4} cL$. The magnetic Prandtl number, $P_m = \nu/\lambda$, is kept fixed to a minimum value of $P_m = 0.1$. The time step is always controlled by the Courant condition $\delta t = 0.25\,\delta x/(c_n^2 + v_{\rm Ai}^2)^{1/2}$, where the numerical factor is determined by accuracy considerations for the scheme and $v_{\rm Ai}$ is the Alfvén speed in the ionized component. Magnetic diffusion and viscosity are too small to affect the time step. We have chosen the most stringent of several possible time step conditions; in particular, the fluid velocities never become large enough to compete with the magnetosonic speeds.

Important timescales in the problem are the ohmic and ambipolar diffusion times,

$$\tau_\Omega = L^2/\lambda , \quad \tau_{\rm AD} = L^2/\lambda_{\rm AD} , \quad (13)$$

where $\lambda_{\rm AD} = B_0^2/(4\pi\gamma\rho_{i0}\,\rho_{n0})$ is the ambipolar diffusion coefficient with respect to the outer values of the densities and the magnetic field, the ionization/recombination timescales

$$\tau_{\rm ion} = (\zeta\rho_{n0}/\rho_{i0})^{-1} , \quad \tau_{\rm rec} = (\alpha\rho_{i0})^{-1} , \quad (14)$$

and the acoustic and Alfvén timescales for ions and neutrals

$$\tau_{ci} = L/(2c_i) , \quad \tau_{cn} = L/c_n , \quad \tau_{\rm Ai} = L/v_{\rm Ai} , \quad \tau_{\rm An} = L/v_{\rm An} , \quad (15)$$

where $v_{\rm Ai} = B_0/(4\pi\rho_{i0})^{1/2}$ and $v_{\rm An} = B_0/(4\pi\rho_{n0})^{1/2}$. The parameter regime of interest is

$$\rho_{i0}\, c_i^2 \ll B_0^2/(4\pi) \ll \rho_n c_n^2 . \quad (16)$$

Thus, we put $c_n = 1$ and $B_0^2 = 4\pi$, which gives the dimensions for the velocity and magnetic field.

It is worth noting that the second inequality in equation (16) does not hold globally in the ISM, particularly in molecular clouds. It should be understood that we are looking at a local model of the neighborhood of a neutral sheet, so the gas pressure is certainly expected to dominate over some range.

We vary c_i between 2.0 and 1, and put $\rho_{i0} = 0.1$ and $\rho_{n0} = 10$. This density ratio of ions to neutrals is not nearly as small as the ratio in cool H I and cold molecular gas, but computational problems arise if we make ρ_i too small, so we hope that the value adopted is low enough to see effects that are typical for weakly ionized media. We furthermore put $L = 1$, which then fixes the units of length and time. Using $\gamma = 1$–100, we have $\tau_{\rm AD} = 1$–100, which is much shorter than the ohmic diffusion time $\tau_\Omega = 4 \times 10^3$. The Alfvén and acoustic times are $\tau_{\rm Ai} = 0.32$, $\tau_{\rm An} = 3.2$, $\tau_{ci} = 0.5$, and $\tau_{cn} = 1$. We vary ζ between 10^{-4} and 10^{-1} and, in order to ensure initial ionization/recombination balance, we put $\alpha = \zeta\rho_{n0}/\rho_{i0}^2$. Thus, $\tau_{\rm ion} = \tau_{\rm rec} = 0.1$–$100$. The mean free path of ions is $l = c_n/\nu_{in} = 10^{-1}$–$10^{-3}$, which is short compared to the macroscopic scales, a point which we return to in § 3.3.

3. RESULTS

3.1. *Oscillations*

Immediately after starting the simulation, we find decaying oscillations in all variables with a period $P \approx 3.8 \pm 0.02$ (for $\gamma = 10$). It is reasonable that there should be oscillatory relaxation, because the initial conditions do not satisfy force balance. For comparison, we solved the dispersion relation for compressive waves with a uniform background magnetic field with B_0 for $k = \pi/2$, i.e., the lowest wavenumber consistent with the boundary conditions. Both frequencies and decay rates agree well with the numerical solution for a nonuniform field. In the absence of a magnetic field, these oscillations still exist as purely acoustic oscillations of the neutrals. In Table 1 we compare the decay rates obtained from the numerical solution and from the dispersion relation (denoted by approximation).

In the parameter range investigated, we find that the amplitudes of the five variables scale according to the following approximate relation:

$$\frac{\delta B}{B_0} \approx \frac{\delta u_i}{c_n} \approx \frac{\delta u_n}{c_n} \approx \frac{\delta \rho_i}{\rho_i} \approx \frac{\delta \rho_n}{\rho_n} . \quad (17)$$

The decay rate is of the order of the ambipolar diffusion time, but it does not scale linearly with $\tau_{\rm AD}$, which is in agreement with the dispersion relation (see Table 1).

In Figure 1 we show the oscillations of all five variables (at $z = 0.5$) about their mean value. Note that the velocities advance the magnetic field by $\pi/2$, whereas the densities are in

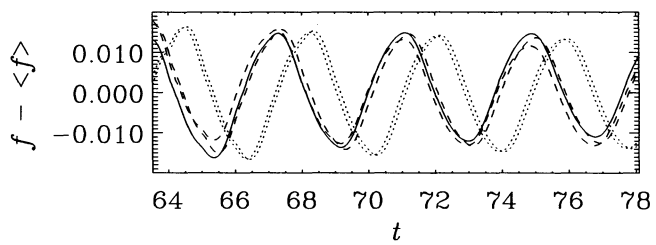

FIG. 1.—Oscillations of all five variables (at $z = 0.5$) about their mean value. $\zeta = 10^{-3}$, $\gamma = 10$ (run B0). Here f stands for one of the terms in eq. (16). Solid line is for $\delta B/B_0$, dotted lines are for u_i/c_n and u_n/c_n, and dashed lines are for $\delta \ln \rho_i$ and $\delta \ln \rho_n$.

TABLE 1

SUMMARY OF THE RUNS AND COMPARISON WITH APPROXIMATION

							Numerical Solution				Approximation			
Run	γ	$\log \zeta$	c_i	c_n	ρ_{i0}	R_m^{grid}	B_*	z_1	ρ_i^*/ρ_{i0}	τ^{-1}	B_*	z_1	ρ_i^*/ρ_{i0}	τ^{-1}
A0	10	−1	1	1	0.1	4	0.47	0.004	1.6	0.015	0.53	0.005	1.7	0.010
A1	10	−1	1	1	0.1	1	0.31	0.011	1.3	0.011	0.40	0.013	1.4	0.010
B0	10	−3	1	1	0.1	4	0.88	0.021	3.0	0.014	0.89	0.023	3.0	0.013
B1	10	−3	1	1	0.1	1	0.80	0.047	2.6	0.015	0.81	0.052	2.7	0.013
B2	1	−3	1	1	0.1	4	0.99	0.018	3.4	0.038	0.99	0.020	3.4	0.038
B3	100	−3	1	1	0.1	4	0.49	0.037	1.6	0.002	0.53	0.045	1.7	0.002
C0	10	−3	0.5	1	0.1	4	0.75	0.010	6.7	0.009	0.76	0.010	6.7	0.010
C1	10	−3	0.5	1	0.1	1	0.63	0.023	5.0	0.010	0.64	0.026	5.1	0.010
D0	10	−3	1	2	0.1	4	0.85	0.031	2.8	0.003	0.86	0.034	2.8	0.002
E0	10	−4	1	1	0.1	4	0.96	0.061	3.3	0.012	0.96	0.064	3.3	0.013
E1	10	−4	1	1	0.1	1	0.92	0.117	3.1	0.012	0.93	0.135	3.2	0.013
F1	10	−3	1	1	0.02	1	0.74	0.007	7.9	0.034	0.75	0.007	8.0	0.038

NOTE. The e-folding time of the oscillations, τ, is compared with the approximation obtained by solving the dispersion relation for a uniform magnetic background field.

phase with the magnetic field. The neutral velocity advances the ion velocity by a very small amount (see the two neighboring dotted lines), and similarly the neutral density advances the ion density. This sign of phase shift is to be expected for magnetosonic waves in weakly ionized gas. For smaller values of γ (i.e., stronger ambipolar diffusion) this phase lag becomes larger and close to $\pi/2$.

3.2. *Asymptotic Scaling Properties*

In this section we investigate scaling properties of various quantities and compare the numerical results with analytical approximations. The various runs are summarized in Table 1, and the solutions are parameterized in a way that is explained below.

It is very time consuming to solve until we obtain a truly steady state. Therefore we consider quantities that are averaged over two periods. We are secure in doing so because, as discussed in the preceding section, we have verified that the oscillations are not caused by numerical errors but are frictionally damped magnetosonic waves. Furthermore, we show in § 3.4 that there is a reduced set of equations for the ions which lead to the steady state that we now describe, without oscillatory behavior.

On average, the center of mass does not change, so we have

$$\bar{\rho}_i \bar{u}_i + \bar{\rho}_n \bar{u}_n \approx 0 \,. \tag{18}$$

Since $\rho_i \ll \rho_n$, $\bar{u}_n$ is small compared with $\bar{u}_i$ (but only on average!) and will be neglected for the current discussion. (In the numerical computations it is, of course, always included.) A comparison of the two profiles is given in Figure 2.

Sufficiently far away from the origin resistive effects will be unimportant, and we expect asymptotic scaling properties. The ion pressure is only important near the origin and can be neglected in the asymptotic regime; see Figure 3. Thus, on average, we expect a balance between the Lorentz force and the drag resulting from elastic collisions between ions and neutrals as well as the momentum transfer associated with ionization and recombination. From equation (9), we then obtain

$$\bar{u}_i \approx -\frac{\bar{B}}{\bar{\rho}_i \bar{\nu}_{in}} \frac{\partial \bar{B}}{\partial z} \,. \tag{19}$$

Here we have assumed that $\zeta \bar{\rho}_n \ll \bar{\rho}_i \bar{\nu}_{in}$. If that is not the case (for example, in run A0, where $\zeta \bar{\rho}_n = 0.1 \bar{\rho}_i \bar{\nu}_{in}$), we have to replace $\bar{\rho}_i \bar{\nu}_{in} \to \bar{\rho}_i \bar{\nu}_{in} + \zeta \bar{\rho}_n$.

In the steady state, or on average, the electric field is constant, ie., $\bar{u}_i \bar{B} = -E$, where E itself is positive. Using equation (18), and integrating over z, we obtain

$$\bar{B}^3 = B_0^3 + 12\pi E \bar{\rho}_i \bar{\nu}_{in}(z - L) \,, \tag{20}$$

which clearly satisfies the outer boundary condition. It is convenient to rewrite $\bar{B}$ in the form

$$\bar{B} \approx B_*(1 + z/z_*)^{1/3} \,, \tag{21}$$

where $\bar{B} = (B_0^3 - 12\pi E \bar{\rho}_i \bar{\nu}_{in} L)^{1/3}$ is the value of $\bar{B}$ extrapolated to $z = 0$, and $z_*/L = [(B_0/B_*)^3 - 1]^{-1}$ is the (negative) value of z at which the extrapolated value of $\bar{B}$ would go through zero. The asymptotic form of the ion velocity is

$$\bar{u}_i \approx u_{i*}(1 + z/z_*)^{-1/3} \,, \tag{22}$$

where $u_{i*} = -B_*^2/(12\pi z_* \bar{\rho}_i \bar{\nu}_{in})$.

In Figure 4*a* we show the profile of B^3 versus z, illustrating that the $\bar{B} \propto (z + z_*)^{1/3}$ scaling is indeed well reproduced. Note, however, that there is a marked "offset" between the outer solution and the origin such that the magnetic field profile becomes even sharper than the ideal $z^{1/3}$ solution (at

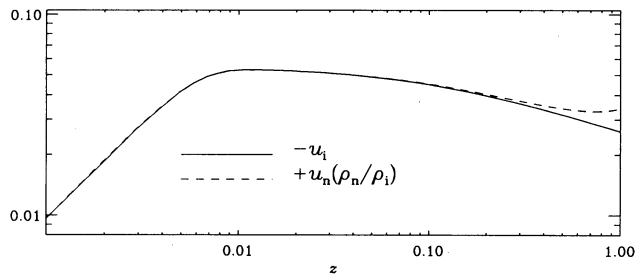

FIG. 2.—Comparison of the averaged ion and neutral velocities for $\gamma = 10$ and $\zeta = 0.1$ (run A0). Deviations occur near $z = 1$.

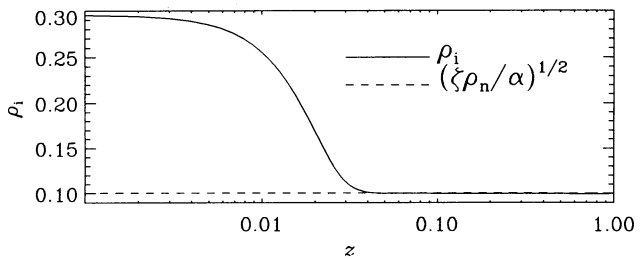

FIG. 3.—Profile of ion density and comparison with $(\zeta\rho_n/\alpha)^{1/2}$ for run B0

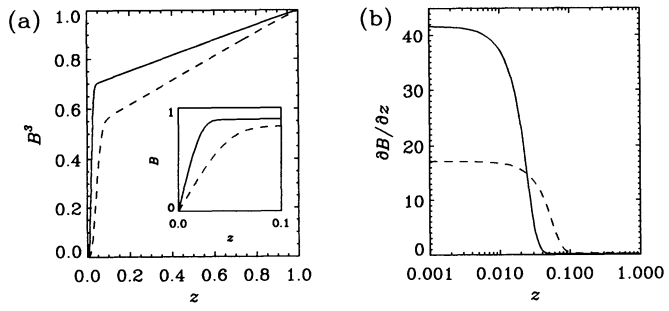

FIG. 4.—(*a*) Profile of $\bar{B}^3$ vs. z for two different values of the ohmic diffusion (*solid line*, $R_m^{\rm grid} = 4$; *dashed line*, $R_m^{\rm grid} = 1$). The inset shows B vs. z in the inner part ($0 \le z \le 0.1$). Note the crossover from diffusive scaling (near $z = 0$) to the ambipolar diffusive scaling (*linear slope*). (*b*) The corresponding current density $\partial\bar{B}/\partial z$ for runs B0 and B1.

least some distance away from $z = 0$). This offset is measured by the quantity B_* (see also Table 1). In order to understand this somewhat surprising behavior and to predict its value for given input parameters, we need to match the asymptotic (outer) solution to the inner solution that is valid near the origin.

3.3. *Matching the Solution near the Origin*

Near the origin, where the ion velocity must go to zero, magnetic diffusion must dominate induction in order to keep the electric field, $E = -\bar{u}_i \bar{B} + \lambda\,\partial\bar{B}/\partial z$, uniform. Sufficiently close to the origin we have $\lambda\partial\bar{B}/\partial z = E$, and the solution that satisfies the inner boundary condition $B(0) = 0$ is therefore

$$\bar{B} = (E/\lambda)z \equiv B_1 z/z_1 \,. \tag{23}$$

Requiring now that the two solutions (20) and (21) match at the transition point $z = z_1$, we can eliminate E and obtain

$$z_1 = 3L\,\frac{\lambda}{\lambda_{\rm AD}}\,\frac{b}{1-b^3}\,, \tag{24}$$

where $b = B_1/B_0$ is the normalized magnetic field at the transition point. Here we have assumed $z_1 \ll L$, which is satisfied in the (for us) relevant case where $\lambda \ll \lambda_{\rm AD}$.

In order to fix the value of z_1, we need another relation between B_1 and z_1. Let us therefore recall that there are two effects that prevent the asymptotic $(z + z_*)^{1/3}$ solution from extending all the way to the origin. Both ohmic diffusion itself and the buildup of ion pressure prevent the ion velocity from becoming singular at the origin (see also Fig. 2). In the complete absence of ion pressure, resistivity alone would make the magnetic pressure gradient, and thus u_i, linear at the origin. We will see that when the parameters of the problem take values appropriate to the interstellar medium, ion pressure is large enough to decelerate the flow outside the region where resistivity would dissipate the current. However, once the flow is decelerated, resistive effects begin to compete with inductive effects. This means that both resistivity and pressure gradients together determine the shape of the final solution.

In Figure 5 we see that the magnetic pressure gradient is balanced by the ion pressure gradient near the origin, and by the ion-neutral collisions away from the origin. Near the origin we can therefore estimate the ion density by

$$\frac{\bar{\rho}_i}{\rho_{i0}} \approx 1 + \frac{b^2}{\beta}\left[1 - \left(\frac{z}{z_1}\right)^2\right], \tag{25}$$

where $\beta = 16\pi\rho_{i0}\,c_i^2/B_0^2$ is the plasma beta (at $z = L$) with

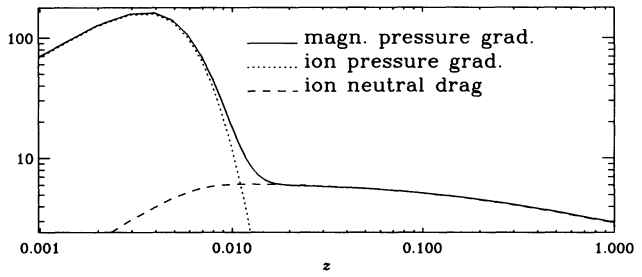

FIG. 5.—Balance of the magnetic pressure gradient by (i) the ion pressure gradient near the origin and (ii) the ion-neutral collisions away from the origin for run A0.

respect to the charged fluid. For the maximum density (see Table 1), we have $\rho_i^*/\rho_{i0} = 1 + b^2/\beta$. The excess of charged particles near the origin is a consequence of the ion inflow. In the steady state, or on average, this convergence of ion velocity can only be compensated by recombination. Integrating equation (4), evaluated at $z = z_1$, and using equation (25), we obtain

$$-u_{i1} = \frac{\zeta\rho_{n0}}{\bar{\rho}_i}\int_0^{z_1}\left[\left(\frac{\bar{\rho}_i}{\rho_{i0}}\right)^2 - 1\right]dz$$

$$= z_1\,\frac{\zeta\rho_{n0}}{\rho_{i0}}\,\frac{4b^2}{3\beta}\left(1 + \frac{2}{5}\,\frac{b^2}{\beta}\right), \tag{26}$$

where $\bar{\rho}_i(z_1) = \rho_{i0}$; see equation (25). At the transition point we have $-u_{i1}B_1 \approx \lambda B_1/z_1$, so we can approximate the ion velocity there by

$$u_{i1} \approx -\lambda/z_1 \,. \tag{27}$$

Combining equations (25)–(27) we obtain a second equation between z_1 and B_1:

$$z_1^2 = \frac{3\beta}{4b^2}\,\frac{\lambda\rho_{i0}}{\zeta\rho_{n0}}\left(1 + \frac{2}{5}\,\frac{b^2}{\beta}\right)^{-1}. \tag{28}$$

From equations (24) and (28) we eliminate z_1 and obtain the equation for b

$$(1-b^3)^2 - \frac{4}{3}\,\frac{Q^2}{\beta^2}\left(\beta + \frac{2}{5}\,b^2\right)b^4 = 0\,, \tag{29}$$

where

$$Q = \frac{3L}{\lambda_{\rm AD}}\left(\lambda\,\frac{\zeta\rho_{n0}}{\rho_{i0}}\right)^{1/2}. \tag{30}$$

The roots of equation (29) give the value of $b = b(Q, \beta)$ at the transition point. It turns out that there is only one real root within $0 \le b \le 1$. In Figure 6 we give the graph of b versus Q for different values of β. In practice, we are most interested in

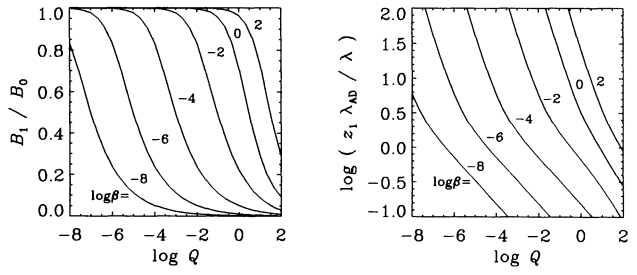

FIG. 6.—Graphs of $B_1 = B_1(Q, \beta)$ vs. Q for different values of β (*left panel*) and $z_1\lambda_{\rm AD}/\lambda$ (*right panel*).

the case $\beta \ll b \ll 1$, $Q/\beta \ll 1$, and then the relevant root of equation (29) is $b \approx 1.11(\beta/Q)^{1/3}$.

Note that Q is governed by the geometrical mean of ohmic diffusion and ionization timescales relative to the ambipolar diffusion timescale. It is illuminating to rewrite Q in terms of basic timescales in the problem. In order to do this we assume that the resistivity η, which is related to λ by $\lambda = (c^2\eta)/4\pi$, is caused by electron collisions with neutrals, which occur at a rate ν_{en}. We take for the collision rate

$$\nu_{en} = 4 \times 10^{-15}\left(\frac{8kT}{\pi m_e}\right)^{1/2} n_n \, \mathrm{s}^{-1} = 2.5 \times 10^{-9} T^{1/2} n_n \, \mathrm{s}^{-1} , \tag{31}$$

where we use the velocity independent cross section given by Krall & Trivelpiece (1973), take $T = 10$ K, and express n_n in cgs units. We compute the ion-neutral collision frequency assuming that HCO^+ and H_2 are, respectively, the dominant ion and neutral species and find, using the collision rates from Draine, Roberge, & Dalgarno (1983),

$$\nu_{in} = 1.3 \times 10^{-10} n_n \, \mathrm{s}^{-1} . \tag{32}$$

We then find that Q can be written in the form

$$Q = 3\tau_{An}\nu_{in}\left(\frac{\nu_{en}}{\omega_{ce}}\frac{\zeta}{\omega_{ci}}\right)^{1/2} = 2.8 \times 10^{-8} n_n^2 L_{\mathrm{pc}} B_\mu^{-2} , \tag{33}$$

where L and B are measured in parsecs and microgauss, respectively, and $\omega_{ce,i}$ are the electron and ion gyrofrequencies. These gyrofrequencies are typically much larger than other frequencies in the problem.

The parameter β is estimated to be

$$\beta = 6.9 \times 10^{-2} n_i B_\mu^{-2} = 7.6 \times 10^{-7} n_n^{1/2} B_\mu^{-2} , \tag{34}$$

where we have used the approximate relation for molecular clouds $n_i \approx 1.1 \times 10^{-5} n_n^{1/2}$ (McKee et al. 1993). We therefore find

$$\beta/Q = 27 n_n^{-3/2} L_{\mathrm{pc}}^{-1} \ll 1 \tag{35}$$

for conditions of interest.

The magnetic profile makes the transition from linear to $z^{1/3}$ scaling at approximately the point z_1. According to equation (24), z_1 is proportional to the ratio $\lambda/\lambda_{\mathrm{AD}}$. In the second panel of Figure 6, the quantity $z_1\lambda_{\mathrm{AD}}/\lambda$ is plotted. Making use of the approximation for $\beta \ll 1$, we have $z_1/L = 3.3(\lambda/\lambda_{\mathrm{AD}})(\beta/Q)^{1/3}$, or

$$\frac{z_1}{L} = 2.9\left(\frac{\tau_{Ai}}{\tau_{ci}}\right)^{2/3}\left(\frac{\tau_{\mathrm{AD}}^4 \tau_{\mathrm{ion}}}{\tau_\Omega^5}\right)^{1/6} = 5 \times 10^3 L_{\mathrm{pc}}^{2/3} n_n^{3/2} B_\mu^{-2} \ \mathrm{cm} , \tag{36}$$

where the unit of length appears on the right-hand side because we are scaling L in parsecs. Note that this scale decreases almost proportionally with λ. For comparison, the skin depth δ, which is the scale that arises from balancing advection and diffusion, i.e., $\delta = (\lambda/Lu_t)^{1/2}$, is proportional to $\lambda^{1/2}$. Using $\lambda = 2 \times 10^8 n_n^{1/2}$, we have $\delta = 2 \times 10^{10} L_{\mathrm{pc}}^{1/2} n_n^{1/4}$ cm, where we assumed for the turbulent velocity $u_t = 10 \ \mathrm{km \ s^{-1}}$.

The scale for z_1 is so small that it cannot be real. Instead of singularity quenching by pressure or resistivity, there must be some effect outside the scope of fluid theory which limits the sharpness of the magnetic profile. Two length scales emerge as likely candidates: the ion mean free path, and the ion gyroradius. The latter is expected to be much smaller; the gyroradius for HCO^+ at $T = 10$ K is $a_i = 1.6 \times 10^7/B_\mu$ cm, where B_μ is the magnetic field in microgauss. Since the ions are tied to the field lines, sharp structure could persist down to these scales much as quasi-perpendicular collisionless shocks exhibit transitions in the fluid properties on scales as small as an ion gyroradius.

The considerations above have illustrated the importance of numerics in testing and motivating analytical scaling relations. The range of different time and length scales relevant to the interstellar medium is so broad that it would be very hard to apply the numerical computations directly to those values. Instead, what we have done here is to use the simulations to identify the relevant balance mechanisms in the system of equations and to obtain clear guidance as to how to construct an approximate relation that would be valid beyond the regime accessible to the numerics, provided of course that no new physics enters.

3.4. *Reduced Equations for the Ions*

In the approximation above, we neglected the dynamics of the neutrals. It is indeed a good approximation to solve just the reduced set of the following equations:

$$\frac{\partial}{\partial z}\left(u_i B - \lambda \frac{\partial B}{\partial z}\right) = 0 , \tag{37}$$

$$\frac{\partial}{\partial z}\left(2\rho_i c_i^2 + \frac{1}{8\pi} B^2\right) = -\rho_i \nu_{in} u_i , \tag{38}$$

$$\frac{\partial}{\partial z}(\rho_i u_i) = \zeta \rho_{n0} - \alpha \rho_i^2 . \tag{39}$$

Although we found it more convenient to solve these equations time dependently and with viscosity included, the solution is much more easily obtained, because the oscillations discussed in § 3.1 are now absent, and we therefore do not need to compute a time average. We repeated runs B0 and F1 and found the same numbers as given in Table 1.

It should be noted that the reduced set of equations for the ions is quite distinct from the usual one-fluid approximation, where one solves for the neutrals in the strong coupling limit. In our one-dimensional model, the breakdown of the strong coupling approximation can affect the solution even far away from the null.

4. MAGNETIC RECONNECTION

We have shown in the preceding section that ambipolar drift in the vicinity of a magnetic null results in large current densities over small scales. We have argued on intuitive grounds that this behavior promotes rapid reconnection, and in this section we quantify that claim. We first show that magnetic field and current profiles of the type seen in Figure 4*b* are indeed unstable to the resistive tearing mode (Furth, Killen, & Rosenbluth 1963, hereafter FKR). We then compute the growth rates and find them to be so large that the time to form the profile, and not the tearing mode time, is the longest timescale in the problem.

The tearing instability can be treated in two dimensions using stream functions for the velocity and the magnetic field. We follow the analysis of White (1983) and express the magnetic field as $\nabla \times \psi\hat{y}$, where

$$\psi(x, z, t) = \psi_0(z) + \psi_1(z) \cos kx \exp \sigma t . \tag{40}$$

(We rely here on pressure instead of a third component of the magnetic field to render the motion incompressible.) In tearing mode theory, the Alfvén and resistive timescales are assumed to be well separated, and resistivity is unimportant outside a thin layer in which the tearing takes place. The condition for instability, however, depends on the equilibrium magnetic profile and can be derived from the differential equation satisfied by ψ_1 in the outer region, in which resistivity is negligible,

$$\psi_1'' = (k^2 + B''/B)\psi_1 , \quad (41)$$

with the boundary conditions $\psi_1 = 1$ at $z = 0$ and $\psi_1 = 0$ for $z \to \infty$. (Here primes denote differentiation with respect to z.) Note that equation (41) has a singular point at $z = 0$ because of the null in B; in fact, the solution must be matched to a solution in the inner region, which includes resistivity.

We solve equation (41) for different values of k. FKR showed that the equilibrium magnetic profile is unstable to tearing if the derivative of ψ_1 at the origin, $\psi_1'(0_+) \equiv \Delta'/2$, is positive (see Adler, Kulsrud, & White 1980 for a demonstration that the free energy available to drive the tearing mode is proportional to Δ'). In a fully ionized medium, the growth rate is given approximately by

$$\sigma_* = \tau_\Omega^{-3/5}(kv_{Ai})^{2/5}\Delta'^{4/5} . \quad (42)$$

In the first panel of Figure 7 we plot Δ' versus k for runs B0 and B1. Referring back to Table 1, we see that these runs have the same parameters except for resistivity, which is 4 times larger for run B1 than for run B0. Evidently the broadened current profile and enlarged linear region in run B1 substantially reduces Δ'.

In all the cases given in Table 1, the growth rate increases with decreasing k. We assume x is bounded by L and impose periodic boundary conditions, requiring $k > k_{min} \equiv 2\pi/L$. In the second panel of Figure 7 we plot Δ' versus z_1 for all runs, assuming $k = k_{min}$. Evidently log Δ' is remarkably well correlated with log z_1; the best fit is $\Delta' = 0.26z_1^{-2}$.

We can now draw the resulting field lines by plotting contours of ψ using equation (40); see Figure 8. We obtain ψ_0 by integrating B. Near the origin we have to match the outer solution ψ_1 to the inner solution. For the purpose of this picture, we fitted the outer solution to a parabola at the turning point of ψ_1.

Applying the tearing mode instability to molecular clouds, the growth rate σ_* can be written as

$$\sigma_* = 1.4 \times 10^{-4} n_n^{1/5} B_\mu^2 (z_1/a_i)^{-8/5} \text{ s}^{-1} , \quad (43)$$

where we have normalized the reconnection scale by the ion gyroradius a_i in view of our remarks at the end of the previous section; z_1/a_i is expected to be of order unity. This growth rate

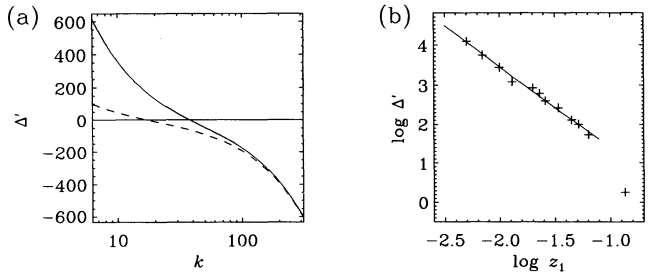

FIG. 7.—(*a*) Δ' vs. k for runs B0 (*solid line*) and B1 (*dashed line*). (*b*) Scatter plot of Δ' vs. z_1 for all runs given in Table 1. Linear fit is $\Delta' = 0.26(z_1/L)^{-2}$.

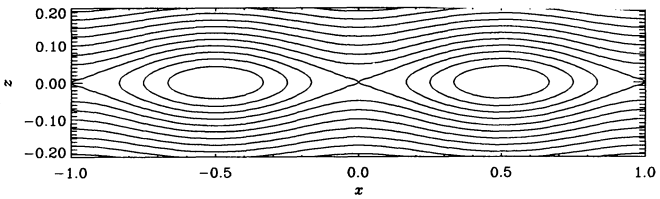

FIG. 8.—Magnetic field lines for run B0

typically exceeds the ion-neutral collision frequency. Therefore ions and neutrals are not well coupled over a tearing mode growth time, and the growth rate is given by σ_* (Zweibel 1989). In fact, the growth rate might be better analyzed by a collisionless theory. In any case, the growth time is so short that the effective time for reconnection in this case is the time it takes to form the nearly singular current profile in the first place, which in this problem is of order $\tau_{AD} \approx 2.5 \times 10^5 n_n^{3/2} L_{pc}^2 B_\mu^{-2}$ yr. In other situations, such as shear flows like the rotating eddy studied in BZ, the timescale could be influenced by dynamics as well.

5. CONCLUSIONS

Magnetic reconnection is thought on phenomenological grounds to occur in a wide variety of astrophysical settings, including collapsing, magnetized interstellar clouds (Mestel 1966; Galli & Shu 1993), interactions between strong poloidal field lines and molecular clouds near the galactic center (Serabyn & Morris 1994), tangled field lines in molecular clouds (Clifford & Elmegreen 1983), and finally, on the largest scale, the galactic dynamo itself. In order to amplify the large-scale magnetic field of the galaxy within its relatively short lifetime, it is crucial that the magnetic field topology can change rapidly on a dynamical timescale and virtually independently of ohmic diffusion. However, only ohmic diffusion can change the field topology, and, in order for this process to be fast, one needs to produce magnetic field gradients at very small scales.

Turbulence can create sufficiently small scales by winding up the field around vortex tubes. This is an important mechanism, especially when the field is not strong enough to counteract this windup process (which can be particularly severe in two dimensions; see Cattaneo & Vainshtein 1991).

The formation of sharp structures by ambipolar diffusion, on the other hand, can in principle be initiated even when the field lines are almost straight, although this then requires the presence of magnetic nulls. In actual turbulence, however, there is always some amount of shear, so that ambipolar ion-neutral drift can create sharp gradients even when there are no perfect nulls; see BZ and Mac Low et al. (1995). These gradients are formed through the action of Lorentz forces on the ions, and, in the example we have studied (BZ), lead to a state in which the field is nearly force-free everywhere except in thin layers of intense current. Very little windup of the field—approximately one rotation—is required to establish the magnetic geometry necessary for this state, suggesting that the mechanism can work even when the field is near equipartition.

Our mechanism of generating sharp structures is somewhat reminiscent of the scenario of hydrodynamic vortex reconnection (Kerr 1993), where antiparallel vortex tubes attract each other until they finally reconnect. Here too there is no windup but, again, in actual turbulence there is always some shear, so that this mechanism will hardly be realized in isolation.

We should point out that linear theory cannot be adopted near nulls. This explains partly why such theory predicts that ambipolar drift damps fluctuations and works against energy transfer to sufficiently small scales (Kulsrud & Anderson 1992).

Although we have demonstrated this only in two dimensions (BZ), we expect that also in three dimensions ambipolar drift acts to make the field force-free ($\boldsymbol{J} \times \boldsymbol{B} \rightarrow 0$), because the ions, having little inertia, quickly respond to Lorentz forces. This has the interesting consequence that it can inhibit dynamo action, because it can be shown from the magnetic induction equation that the growth of magnetic energy is proportional to $\langle \boldsymbol{u} \cdot (\boldsymbol{J} \times \boldsymbol{B}) \rangle$. Therefore, although we pointed out above that ambipolar diffusion might facilitate dynamo action by enhancing the rate of magnetic reconnection, the net effect of ambipolar diffusion on dynamos might not be wholly salutary. In any case, more examples of turbulent MHD flows with ambipolar diffusion are needed to assess the prevalence of the singularity and its effects.

Finally, we would like to reiterate that the strong coupling approximation, which was used in BZ, evidently breaks down near the singularity. Our present investigations have shown, however, that this in no way impedes the formation of sharp structures. Indeed, the more consistent treatment using the two-fluid theory shows that oppositely oriented magnetic fields can be pushed together down to scales shorter than the hitherto known dissipative cutoff scales. Since the fluid approximation breaks down at scales shorter than the gyroradius, we can consider this new scale as virtually zero.

We thank Mark Rast for comments on the manuscripts E. G. Z. is happy to acknowledge support for this work by the NASA Astrophysical and Space Physics Theory Programs.

REFERENCES

Adler, E. A., Kulsrud, R. M., & White, R. B. 1980, Phys. Fluids, 23, 1375
Brandenburg, A., & Zweibel, E. G. 1994, ApJ, 427, L91
Cattaneo, F., & Vainshtein, S. I. 1991, ApJ, 376, L21
Clifford, P., & Elmegreen, B. G. 1983, MNRAS, 202, 629
Draine, B. T. 1986, MNRAS, 220, 133
Draine, B. T., Roberge, W. G., & Dalgarno, A. 1983, ApJ, 264, 485
Furth, H. P., Killen, J., & Rosenbluth, M. N. 1963, Phys. Fluids, 6, 459
Galli, D., & Shu, F. H. 1993, ApJ, 417, 220
Kerr, R. M. 1993, Phys. Fluids, A5, 1725
Krall, N. A., & Trivelpiece, A. W. 1973, Principles of Plasma Physics (New York: McGraw-Hill)
Kulsrud, R. M., & Anderson, S. W. 1992, ApJ, 396, 606
Kulsrud, R., & Pearce, W. P. 1969, ApJ, 156, 445
Mac Low, M.-M., Norman, M. L., Königl, A., & Wardle, M. 1995, ApJ, 442, 726
McKee, C. F., Zweibel, E. G., Goodman, A. A., & Heiles, C. 1993, in Protostars and Planets III, ed. E. H. Levy and J. I. Lunine (Tucson: Univ. Arizona Press), 327
Mestel, L. 1966, MNRAS, 133, 265
Mestel, L., & Spitzer, L., Jr. 1956, MNRAS, 116, 503
Proctor, M. R. E., & Zweibel, E. G. 1992, Geophys. Astrophys. Fluid Dyn., 64, 145
Serabyn, E., & Morris, M. 1994, ApJ, 424, L21
Shu, F. H. 1983, ApJ, 273, 202
Spitzer, L., Jr. 1978, Physical Processes in the Interstellar Medium (New York: Wiley)
White, R. B. 1983, in Handbook of Plasma Physics, ed. M. N. Rosenbluth, & R. Z. Sagdeev (Dordrecht: North-Holland), 611
Zeldovich, Ya. B., & Raizer, Yu. P. 1967, Physics of Shock Waves and High-Temperature Hydrodynamic Phenomena (New York: Academic)
Zweibel, E. G. 1989, ApJ, 340, 550